A structural view of Pd model catalysts : high-pressure surface X-Ray diffraction

Rijn, R. van

Chapter 3

Surface structure and reactivity of Pd(100) during CO oxidation near ambient pressure

The surface structure of Pd(100) during CO oxidation was measured using a combination of a flow reactor and in situ surface x-ray diffraction coupled to a large-area 2-dimensional detector. The surface structure was measured for P_{O_2}/P_{CO} ratios between 0.6 and 10 at a fixed total gas pressure of 200 mbar and a fixed CO pressure of 10 ± 1 mbar. In conjunction with the surface structure the reactivity of the surface was also determined. For all P_{O_2}/P_{CO} ratios the surface was found to oxidise above a certain temperature. Three different types of oxides were observed: the $(\sqrt{5} \times \sqrt{5})R27^\circ$ surface oxide, an epitaxial layer of bulk-like PdO, and a non-epitaxial layer of bulk-like PdO. As soon as an oxide was present the reactivity of the surface was found to be mass transfer limited by the flux of CO molecules reaching the surface.

Published as: *Surface structure and reactivity of Pd(100) during CO oxidation near ambient pressures*,
R. van Rijn, O. Balmes, A. Resta, D. Wermeille, R. Westerström, J. Gustafson, R. Felici, E. Lundgren, and J. W. M. Frenken,
Physical Chemistry Chemical Physics **13**, 13167-13171 (2011).

3.1 Introduction

Detailed knowledge of the atomic structure of catalytically active surfaces under operating conditions is of paramount importance for the full understanding of heterogeneous catalysis on the atomic scale. Since a real catalyst is a complex combination of materials working under high-temperature and high-pressure conditions, it is difficult to measure the surface structure of the active part of the catalyst and thus to obtain an atomic scale understanding of the catalytic process in a straightforward way. Instead, single-crystal surfaces have been used as model systems resulting in significant insight in adsorbate-adsorbate and adsorbate-substrate interactions, especially under ultrahigh vacuum (UHV) conditions [13].

Thanks to a growing number of available experimental techniques developed to study surfaces in ambient pressure environments, atomic scale insight is nowadays also obtained under semi-realistic operating conditions [14, 16, 23]. Examples of techniques bridging the so-called pressure gap are transmission electron microscopy (TEM) [53], high-pressure scanning tunnelling microscopy (STM) [54], x-ray photoelectron spectroscopy (XPS) [55], sum frequency generation (SFG) [56], and surface x-ray diffraction (SXRD) [57]. Each of these techniques has different abilities in probing either the reactants on the surface or the surface structure of the active catalytic material. SXRD is inherently sensitive to the atomic scale surface structure, also at gas pressures beyond several bars, making it an excellent technique to study phase changes in the catalyst under realistic reaction conditions.

Pd is an important oxidation catalyst, e.g., in the cleaning of automotive exhaus gases and in methane combustion [58, 59]. Modern low-fuel-consumption automotive engines operate under oxygen excess, resulting in oxygen-rich exhaust gases reaching the Pd-based catalyst, which has increasingly motivated studies of the oxidation of Pd under these oxygen rich conditions.

It has been shown that two different oxide phases may form on the Pd(100) surface, depending on the pressure and temperature conditions. One phase is a well-ordered purely 2-dimensional (2D) structure, the $(\sqrt{5}\times\sqrt{5})$R27° phase and the second a 3D epitaxial bulk-like PdO film [49, 60–66]. The experimental determination of the surface phase diagram in pure oxygen indicates that the surface oxide kinetically hinders the formation of the bulk oxide at low temperatures [67]. It was also shown experimentally that the appearance of oxide structures

coincides with an increase in activity of the surface towards CO oxidation as compared to the reactivity on the non oxidized surface [51]. DFT calculations confirm the stability and the activity towards CO oxidation of PdO [68, 69] and the $(\sqrt{5} \times \sqrt{5})$R27° surface oxide [70, 71]. The thermodynamic phase diagram as calculated by DFT shows that under the experimental pressure and temperature conditions applied in this study the thermodynamically stable phase is the $(\sqrt{5} \times \sqrt{5})$R27° surface oxide, whereas bulk PdO only becomes the thermodynamically stable phase at extremely high P_{O_2}/P_{CO} ratios [70]. Moreover the bulk-like PdO layer was shown to play an important role in spontaneous reaction oscillations [72]. However the recent suggestion that the CO oxidation reaction is most efficient, even 'hyperactive', when the surface is in a metallic state that is transient in nature [73], provoked a lively discussion [74–76].

Here we present a high-pressure SXRD study mapping out the structure of the Pd(100) surface under various mildly to very oxidizing P_{O_2}/P_{CO} ratios and different temperatures, realistic conditions for CO oxidation. A combination of a flow reactor and in situ SXRD employing a 2D pixel detector was used. The experiments were conducted under steady state flow conditions, ruling out any transient effects. This allowed us to map out the stability of the metallic Pd(100) surface and the oxide phases under the variety of gas pressures and temperature conditions and under the influence of the catalytic reaction. The mapping resulted in a concise diagram that will be compared to theoretical predictions and other experimental data. In addition to the surface structure we also monitored the CO_2 production at each point in the phase diagram. We observe the highest CO_2 production when an oxide phase is present on the Pd(100) surface. Conclusions about differences in the reactivity of the different oxides could not be drawn and we will explain that this is due to limitations of mass transfer of CO to the sample.

3.2 Experimental methods

The experiments were carried out at the ID03 beamline of the European Synchrotron Radiation Facility (ESRF) [77]. The beamline is equipped with a combined UHV-high pressure flow setup that can be mounted on a six-circle diffractometer [78]. This setup allows for the cleaning of samples in UHV combined with flow experiments in a 13 ml flow cell at reactant pressures up to 1200 mbar.

A beryllium dome functions as part of the reactor wall allowing for entrance and exit of the x-rays. The sample was subjected to several cycles of 1000 eV Ar^+ ion bombardment for 45 minutes and annealing up to 1300 K for 10 minutes. A focused x-ray beam of 18 keV (2×10^{12} photons/s, 80 mA ring current) impinging on the surface under a 1° incidence angle was used for the diffraction experiments. We describe the Pd crystal lattice with a tetragonal unit cell with two vectors in the surface plane ($|\overrightarrow{a_1}| = |\overrightarrow{a_2}| = a_0/\sqrt{2}$) and one perpendicular to the surface plane ($|\overrightarrow{a_3}| = a_0$) where $a_0 = 3.89$ Å. A maxipix 2D pixel detector was used to collect the diffracted x-rays [79–81], allowing for the detection of an area of reciprocal space without having to scan the detector. Each image required less than one second of exposure time and a readout time of 0.29 ms.

A ball model of the two oxide structures is shown in Fig. 3.1a. The $(\sqrt{5} \times \sqrt{5})$R27° phase is described in ref. [61] as a 2D structure, i.e. a single oxide layer, which is essentially a distorted PdO(101) plane. The bulk-like PdO structure usually grows 2-3 nm thick under our experimental conditions with the PdO(101) plane epitaxial to the Pd(100) surface and is thus a 3D structure [49, 62, 64].

One domain of the in-plane reciprocal lattices of both oxide structures is shown in Fig. 3.1b. Due to the p4mm symmetry of the Pd(100) surface and the pm symmetry of the oxide phases, eight domains of orientation of both oxide phases exist on the Pd(100). From Fig. 3.1b one sees that both structures have diffraction features at the (0.4, 0.8, L) and equivalent positions in reciprocal space . Due to the 3D nature of the PdO overlayer one expects a diffraction peak in the L directions at the (0.4, 0.8, 0.74) position of the Pd(100) reciprocal lattice [67]. By choosing this position for the 2D detector we record a region on the Ewald sphere around this position, see Fig. 3.2a. If the 2D $(\sqrt{5} \times \sqrt{5})$R27° structure is present, we expect no peaks along the L direction, but rather a truncation rod of slowly decaying intensity as L is increasing. Figure 3.2b,c show the characteristic signal of the different oxide phases on the detector, confirming these expectations. Note that the peak in Fig. 3.2c for the bulk-like oxide is extended in the L direction compared to the field of view of the 2D detector due to the fact that the layer is just nanometers thick. Under some conditions a third phase was observed consisting of a regular PdO layer that had partially lost its epitaxial orientation to the surface, resulting in PdO powder ring diffraction on the detector, as shown in Fig. 3.2d.

The stability diagram was determined as follows. The clean sample was exposed to a flow as 50 mln/min consisting of a mixture of CO, O_2 and Argon at

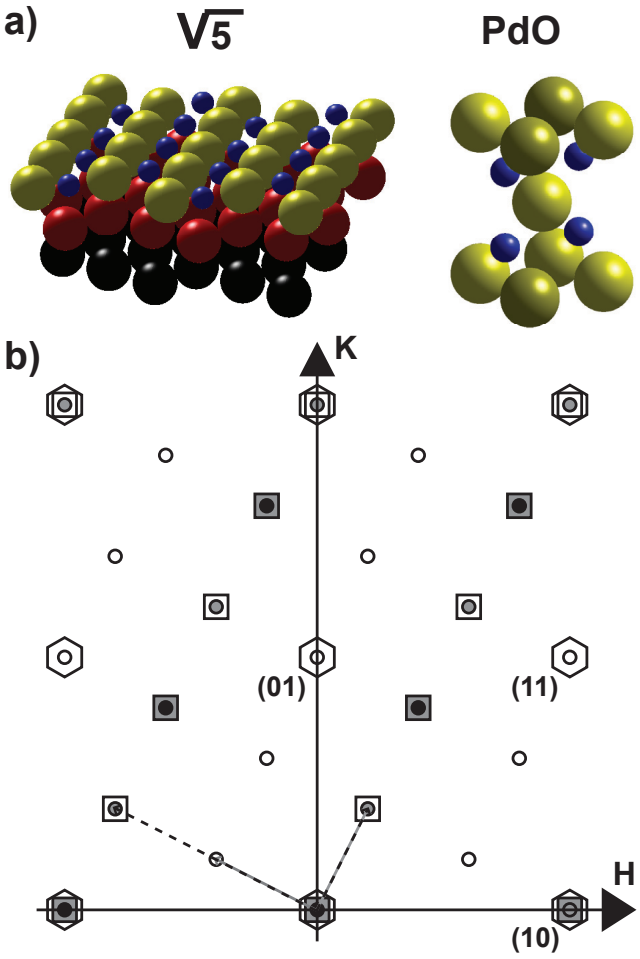

Figure 3.1: a) Left: Ball model of the $(\sqrt{5} \times \sqrt{5})R27^\circ$ phase, blue balls indicate O atoms, yellow, red and black are the first second and third layer of Pd atoms, respectively. Right: Bulk PdO unit cell, blue balls indicate the O atoms and yellows balls indicate Pd atoms.**b)** In-plane reciprocal lattice expressed in reciprocal lattice units of the Pd(100) surface unit cell. Hexagons denote the in-plane reciprocal lattice positions of Pd truncation rods, squares denote the in plane reciprocal lattice of PdO with the PdO(101) face epitaxial to the Pd(100) surface (filled grey squares indicate truncation rods with high intensity reflections, empty squares indicate truncation rods with lower intensity reflections), circles show the in plane reciprocal lattice of the $\sqrt{5} \times \sqrt{5})R27^\circ$ phase (open circles denote negligible intensity, filled grey circles denote measurable intensity, filled black circles show the strongest intensity)

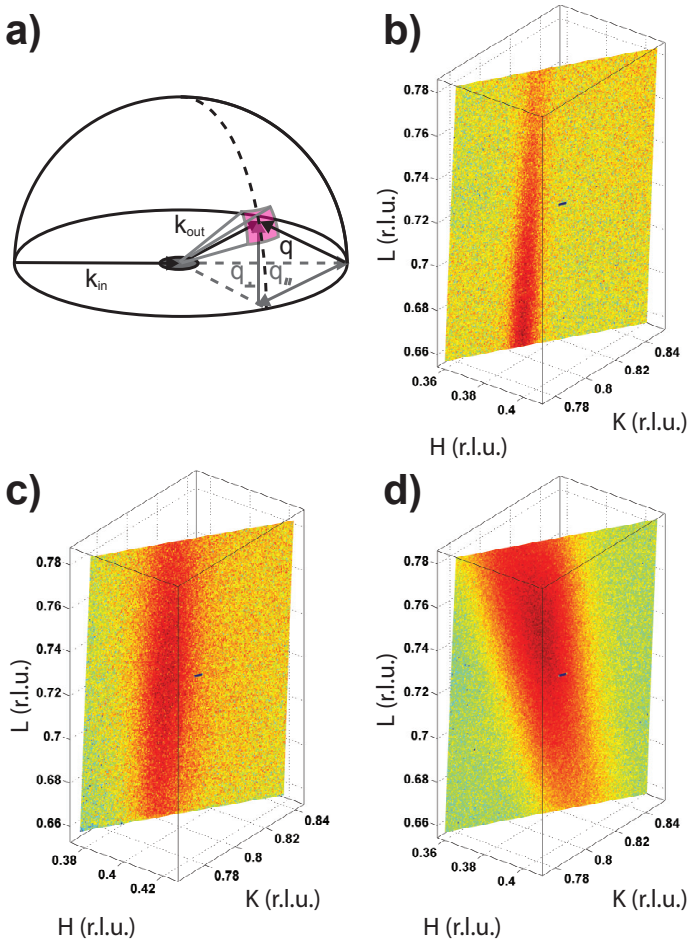

Figure 3.2: a) Surface x-ray diffraction geometry. Note that a spatially resolved diffraction signal is recorded over part of the Ewald sphere by using a 2D detector [81]. The specific cut that the detector makes in reciprocal spaces depends on the incoming X-ray wavelength (radius of the Ewald sphere) and the position of the detector. **b)** Typical intensity profile on detector signifying the presence of the $(\sqrt{5}\times\sqrt{5})$R27° phase, the peak has a small FWHM in the HK plane, indicating the long range order in the plane. **c)** Typical intensity profile associated with an epitaxial bulk-like PdO(101) layer. The relatively broad peak indicates this structure is less well ordered than the $(\sqrt{5}\times\sqrt{5})$R27° phase. **d)** Intensity profile of a bulk-like PdO(101) layer that partly lost epitaxy to the underlying surface. The H, K, and L coordinates are expressed in reciprocal lattice units (r.l.u.) of the underlying Pd(100) surface.

a pressure of 200 mbar, while being heated to the desired temperature. The partial pressure of CO, P_{CO} was kept constant at 10 $\pm$ 1 mbar. The Argon and O_2 pressures were varied to obtain the desired P_{O_2}/P_{CO} ratio, while keeping the total pressure constant. The total pressure was kept constant using Argon to keep the diffusion constant of CO and the heat conduction properties of the gas stream as constant as possible over the whole range of experimental conditions. The surface was allowed to stabilize for several minutes while the diffraction features at the (0.4, 0.8, 0.74) were monitored. Upon obtaining a stable structure, the gas flow was stopped, effectively turning the flow reactor into a batch reactor. The initial slope of the increase of the signal at a mass of 44 amu (the mass of CO_2) in the quadrupole mass spectrometer (QMS) was used to determine the reaction rate of the sample. Subsequently the flow was started again with P_{CO}=P_{Ar}=100 mbar and P_{O_2}=0 mbar to reduce any oxides that might have formed. After confirming that any oxides were reduced, the experiment was repeated for other P_{O_2}/P_{CO} ratios and temperatures.

3.3 Results and discussion

Figure 3.3 shows the resulting stability diagram. By comparing the diffraction features in the image with the three examples in Fig. 3.2, several trends can be observed. First of all the black line marking the metal/oxide stability boundary slopes to the right, i.e. at lower temperature one needs a higher P_{O_2}/P_{CO} ratios to form an oxide on the surface. Second, the $(\sqrt{5}\times\sqrt{5})$R27° surface oxide forms at high temperatures and low P_{O_2}/P_{CO} ratio, while at higher P_{O_2}/P_{CO} ratios the bulk-like PdO oxide forms. This observation is in agreement with studies using pure oxygen to oxidise the Pd(100) surface [67]. However DFT indicates that the bulk-like oxide should not be observed at all under the present conditions [70]. We speculate that this discrepancy is due to the reaction-induced roughness [72] that may locally stabilize the bulk oxide under conditions for which on a flat surface the $(\sqrt{5}\times\sqrt{5})$R27° structure would have the lower energy. Third, the surface tends to form a relatively perfect structure (small FWHM of the peak in the image) $(\sqrt{5}\times\sqrt{5})$R27° at low P_{O_2}/P_{CO} ratios and high temperatures. The FWHM of the oxide is relatively large at high P_{O_2}/P_{CO} compared to lower P_{O_2}/P_{CO} ratios, showing that there is only short-range order present in this PdO layer. In addition, at high P_{O_2}/P_{CO} ratios a PdO film is formed that partly

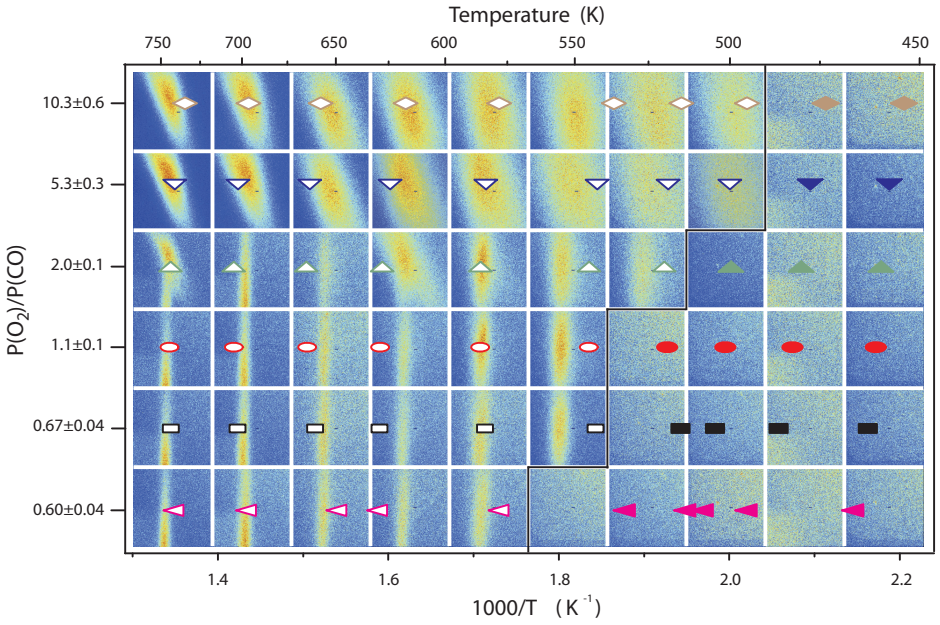

Figure 3.3: Recorded diffraction signal as a function of P_{O_2}/P_{CO} ratio and sample temperature. The total gas pressure in the reactor was kept constant at 200 mbar, the partial CO pressure was kept constant at 10 ± 1 mbar. Oxygen and Argon where mixed in the flow to obtain the desired P_{O_2}/P_{CO} ratio. The different oxides signals introduced in Fig. 3.2 can be recognized. The overlaying symbols indicate the precise temperatures at which the underlying images were obtained. The corresponding values for the CO_2 production are plotted using the same symbols in Fig. 3.4. Open symbols denote the presence of an oxide, filled symbols denote that the surface was metallic in nature. The thick black line indicates the boundary between the metallic and oxidic phases.

lost epitaxy to the substrate. The fact that the $(\sqrt{5} \times \sqrt{5})$R27° structure exhibits a well-ordered 2D structure while the bulk PdO oxide is poorly ordered is in agreement with previous oxidation studies [64, 65]. Fourth, we clearly observe the coexistence of the $(\sqrt{5} \times \sqrt{5})$R27° structure and the bulk-like PdO film that lost epitaxy to the surface for example at T=750 K and T=625 K and P_{O_2}/P_{CO}=2 in Fig. 3.3. The gradual transition from the epitaxial bulk-like oxide of Fig. 3.2c to the $(\sqrt{5} \times \sqrt{5})$R27° of Fig. 3.2b that can be seen in the stability diagram in Fig. 3.3 in the range $600 < T < 650$ and $P_{O_2}/P_{CO} \leq 1.1$ is evidence for the coexistence of these two phases in that pressure and temperature range. The phase

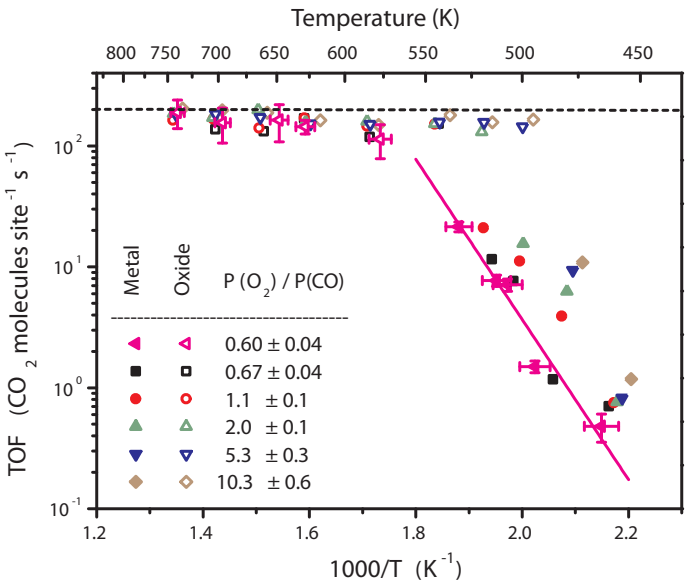

Figure 3.4: Arrhenius plot of the CO_2 production rate over Pd(100) at different P_{O_2}/P_{CO} ratios. The total gas pressure in the reactor was kept constant at 200 mbar, the partial CO pressure was kept constant at 10 ± 1 mbar. Oxygen and Argon where mixed in the flow to obtain the desired P_{O_2}/P_{CO} ratio. Representative error bars and a fit of the Arrhenius behavior are shown for the P_{O_2}/P_{CO}=0.6 data set. The surface structure was determined simultaneously with the TOF by surface x-ray diffraction. Open symbols denote where the SXRD measurements showed the presence of an oxide (surface oxide, bulk-like oxide, or powder pattern) and solid symbols indicate under which conditions SXRD measured an oxide-free metal surface.

coexistence is likely not a pure thermodynamical coexistence, but may extend over a large range due to the presence of kinetic effects (reduction of PdO by CO, diffusion, kinetic hindrance). Also note that for higher temperatures (∼1100 K) than obtainable in this study one would expect the oxides to become thermodynamically unstable again, even in the presence of pure oxygen.

The turnover frequency (TOF) corresponding to the data in Fig. 3.3 are shown in Fig. 3.4 in Arrhenius form. The data splits up into two sets of data points. The first set are the filled symbols were the surface was metallic in nature and the TOF increased with increasing temperature. The second set are the open symbols were the TOF has reached a plateau and does not vary with temperature. The

activation energy on the metal, as determined from the slope of the Arrhenius plot for the P_{O_2}/P_{CO} ratio of 0.6, is 1.32 ± 0.16 eV, in agreement with the value found previously [82]. The data also shows that the TOF was always at the maximum when the surface was oxidized. Our diffusion calculations indicate that the reactivity in this regime was not determined by the intrinsic reactivity of the catalyst, but by the rate at which reactant molecules could be supplied to the catalyst, i.e. by the mass transfer limitation (MTL) of the flow reactor. A first-principles calculation confirms the importance of heat and mass transfer effects [83]. Since our P_{O_2}/P_{CO} ratio was larger than 0.5 and almost all the CO is consumed once the TOF reaches the MTL, the P_{O_2}/P_{CO} ratio at the sample was higher than what was set upstream. This effect is always present, but can be mitigated to a small extent by using small samples, a large flow, or by mixing the gas in the reactor efficiently. Our efforts to increase the flux of CO molecules impinging on the surface by reducing the sample size from a 7 mm diameter to a 1 mm diameter resulted in an oxidation of the surface at a $\sim$50K higher temperature. The MTL was reached again for this small sample as soon as an oxide was present on the surface. The exact conditions under which the sample oxidises thus moderately depend on sample size via the MTL associated with this sample size. This raises the question if the oxidation is the *cause* of the higher reactivity or merely the *effect* of the changing P_{O_2}/P_{CO} ratios at the surface as the temperature is increased and the metallic surface becomes more reactive. The present data does not allow us to directly conclude either way, but we may conclude that all oxides were reactive enough to sustain a mass transfer limited TOF. Since the gas conditions at the sample are net oxidizing the oxide is the thermodynamically stable termination of the Pd(100) surface, as confirmed by DFT calculations [71]. We therefore think it is highly unlikely that any other non-oxidic phase (chemisorbed oxygen, bare metal) would still be present under these conditions, and be responsible for the observed reactivity.

Our observation of the $(\sqrt{5} \times \sqrt{5})$R27° structure at P_{O_2}/P_{CO} ratios from .6 to 1.1 in the stability diagram supports the theoretical predictions that this phase is indeed stable up to stoichiometric reactant feeds [70, 71]. This observation is at odds however, with the claimed absence of the surface oxide in IRAS experiments under similar gas and temperature conditions [73, 76]. This discrepancy raises the question if the $(\sqrt{5} \times \sqrt{5})$R27° phase can be clearly observed in IRAS experiments, either indirectly through the stretch frequency of adsorbed CO or directly through a perpendicular component of the Pd-O vibration, a question also

asked by the authors of ref. [76]. The fact that our CO_2 production is mass transfer limited when the $(\sqrt{5}\times\sqrt{5})$R27° phase is present supports the prediction that this phase is 'clearly not 'inactive' towards CO oxidation' [71]. The high activity of all the observed oxide phases is in line with recent DFT calculations activation energies and efficient reaction pathways on various terminations of PdO [69].

In summary we have shown that the Pd(100) surface oxidizes above a certain temperature under reaction conditions at all P_{O_2}/P_{CO} ratios between 0.6 and 10 at a total gas pressure of 200 mbar. The 2D detector used in our SXRD measurement allowed for relatively fast mapping of reciprocal space, enabling a structural separation between surface, bulk-like and non-epitaxial Pd oxides. Although these oxides appear more reactive than a metallic Pd(100) surface, the MTL of our experimental setup inhibits the detection of differences in the reactivity of the oxides. The good agreement between experimental and theoretical studies however supports a high activity for CO oxidation on the PdO surface.